
Effect of Swirl in a Constant Speed DI Diesel Engine using Computational Fluid Dynamics

R. Thundil Karuppa Raj¹ and R. Manimaran^{2*}

¹ Energy Division, School of Mechanical and Building Sciences,
Vellore Institute of Technology, VIT University, Vellore
Tamilnadu-632014, INDIA

² Thermal and Automotive Division, School of Mechanical and Building Sciences,
Vellore Institute of Technology, VIT University, Vellore
Tamilnadu-632014, INDIA

Received: 23/07/2012 – Revised 22/10/2012 – Accepted 26/11/2012

Abstract

Diesel combustion appears to be the most prominent way to improve fuel efficiency for global CO₂ emissions reduction. To achieve this, the combustion inside the cylinder should be studied and the pollutant emissions, especially NO_x and soot, need to be considered simultaneously. Over the past, substantial advances have been made in the modeling of combustion in direct injection diesel Engines and the progress is attributed to the development of a new model, which take into account explicitly all the described phenomena. In the current work, the operating characteristics of direct injection diesel engine is studied using Extended Coherent Flame Model for 3 zones (ECFM-3Z) model in a CFD tool named es-ICE, an expert system for internal combustion engines. The present study is validated with the experimental work performed by Colin et. al. The combustion and emission characteristics are studied by varying the swirl ratio. It is found that in-cylinder pressure and temperature increases with swirl ratio. NO_x emissions increases and soot levels decreases at higher swirl ratio.

Keywords: Direct injection diesel engine; Equivalence ratio; Swirl ratio; Computational Fluid Dynamics; Combustion; Emissions;

1. Introduction

Combustion and fluid flow modeling in an internal combustion engine presents one of the most challenging problems. This is due to large density variations where, the fluid motion inside a cylinder is turbulent, unsteady, non-stationary both spatially and temporally. The combustion characteristics were greatly influenced by the details of the fuel preparation and the fuel distribution in the engine cylinder, which was mainly controlled by the in-cylinder fluid dynamics. The fuel injection introduces additional complexities like two phase flows. Pollutant emissions were controlled by the turbulent fuel–air mixing and combustion processes. A detailed understanding of

* Corresponding Author: R. Manimaran

Email: manimaran.nr@gmail.com Telephone: +91-94457 37752

© 2013 All rights reserved. ISSR Journals

PII: S2180-1363(12)4214-X

these processes is required to improve performance and reduce emissions without compromising the fuel economy. From the literature, several researchers [1,2] performed experimental and numerical studies [3,4] towards the parameter optimization, fluid mechanics and combustion phenomena.

Zhang et al. [5] carried out an experimental study aiming to investigate the effects of combustion chamber geometry on combustion process in an optically accessible direct injection diesel engine. Flame movement behaviors such as the distribution of flame velocity vectors and the averaged flame velocity inside and outside the combustion chamber are measured by means of cross-correlation method. Studies indicate that re-entrant combustion chamber is better than dish chamber. Stephenson et al. [6] conducted a parametric study on the effects of swirl, initial turbulence, oxygen concentration and ignition delay on fuel vaporization, mixing and combustion process. The effects of intake flow field was further investigated by varying the geometry of the intake ports and intake runners in a model dual port direct injection diesel engine in KIVA simulations. The code solves the three dimension conservation equations and uses an improved RNG $k-\varepsilon$ turbulence model. The effect of swirl on emissions is not considered here. Bianchi et al [7] investigated the influence of different initial condition procedures on combustion and emissions predictions in small-bore high-speed direct injection diesel engine. The analysis was performed by using the STAR-CD code for the intake stroke calculation and KIVA for the compression stroke and combustion simulation. Analysis of the evolution of fluid dynamic parameters has revealed that a detailed definition of the initial conditions is required to properly predict the mean and turbulent flow field at the time of injection near TDC. Chen et al. [8] simulated the transient flow for the induction stroke using STAR-CD software and observed that the standard $k-\varepsilon$ model with wall function for description of boundary layer behavior predict the fully turbulent flow inside the cylinder. Payri et al. [9] and Auriemma et al. [10] made in-cylinder measurements under motoring conditions in a light duty diesel engine equipped with a re-entrant bowl in piston combustion chamber. Tangential and radial components of the air velocity were obtained over a crank angle range of 90° above TDC. Estimates of the mean motion, integral time scale and Reynolds shear stress are also found to be comparable with the computational work.

Swirl motion of the air is usually generated due to the design of the intake port. A good intake port design will generate higher swirl and help to improve combustion [11]. When there is swirl in the in-cylinder air, the swirl-squish interaction produces a complex turbulent flow field at the end of compression. This interaction is much more intense in re-entrant combustion chamber geometries [12]. Further, intensification of swirl and turbulence are observed around TDC of compression. Around this time, most of the in-cylinder air is compressed into a smaller diameter combustion chamber. Thus, by conservation of angular momentum, as the radius of rotation reduces, the speed of rotation increases. Intensification of turbulence is due to the highly turbulent squish and reverse-squish motions of the air near TDC of compression. Because of these, usually two peaks in turbulence, one just before TDC and the other just after the TDC, are observed [13]. In re-entrant chambers, the intensification of swirl and turbulence are higher when compared to cylindrical chambers. This leads to more efficient combustion which in turn causes higher NO_x emissions and less soot and HC emissions [14].

In recent years, to investigate many of the above mentioned aspects, computational tools are being significantly used [15]. Overall, optimization of combustion chamber geometry along with swirl and selected spray parameter is the key to reducing pollutant emissions and for better fuel economy [16]. Jayashankara et al. [17] carried out the computational fluid dynamic investigation to

study the effect of fuel injection timing and intake pressure on the performance of a direct injection diesel engine with toroidal combustion chamber configuration. In case of advanced injection timing the soot emissions show increasing trend up to certain crank angle then reverse trend whereas in case of retarded injection timing soot emissions show the reverse trend. The supercharged with inter-cooled cases show lower peak heat release rate and maximum cumulative heat release, shorter ignition delay, higher oxides of nitrogen and lower soot emissions respectively. Prasad et al. [18] observed that highly re-entrant piston bowl and without a central projection was found to be the best for swirl and turbulent kinetic energy intensification around top dead center. Combustion simulations were carried out using the selected geometry and injection timings were optimized to keep oxides of nitrogen levels below those of the baseline case. An injection timing of 8.6° CA BTDC was found to be optimum since it led to a 27 % reduction in oxides of nitrogen emissions and 85% reduction in soot levels as compared to the baseline configuration.

Single and double zone models lack in accuracy during validation and hence improved computational techniques and efficient solver for influencing the application of computational fluid dynamic methods to reciprocating engine models is needed. These methods require movable domain boundaries and compressible/expandable meshes. The sub-models affecting physical processes such as fuel injection, spray formation, evaporation, mixing, ignition, combustion and pollutant formation need to be accommodated in the package. To accomplish all these challenges, a versatile computational fluid dynamics (CFD) package called es-ICE [19] is used here for rapid in-cylinder diesel engine modeling. The Extended Coherent Flame Model (ECFM) is developed to simulate combustion in premixed and diffusion modes. The ECFM model is based on a flame surface density equation which takes into account the wrinkling of the flame front surface by turbulent eddies and a conditioning averaging technique that allows precise reconstruction of local properties in fresh and burned gases even in the case of high levels of local fuel stratification. It is represented by three mixing zones (3Z): a pure fuel zone, a pure air plus possible residual gases zone and a mixed zone. A mixing model is presented to allow progressive mixing of the initially unmixed fuel and air. The ECFM-3Z combustion model has been validated in a comparative work between diesel experiments [20] and this model can be used to study here the effect of swirl on combustion and emissions in the re-entrant combustion chamber of a single cylinder constant speed direct injection diesel engine.

2. Methodology

The equations for conservation of mass, momentum, energy and species are solved respectively in a solver, es-ICE, an expert system for internal combustion engines. The standard k- ϵ model is which the turbulent Reynolds number forms of the turbulent kinetic energy and turbulent dissipation rate equations are used in conjunction with the algebraic 'law of the wall' representation of flow, heat and mass transfer for the near wall region. The ECFM-3Z model is a general purpose combustion model capable of simulating the complex mechanisms of turbulent mixing, flame propagation, diffusion combustion and pollutant emission that characterize modern internal combustion engines. '3Z' stands for three zones of mixing, namely the unmixed fuel zone, the mixed gases zone, and unmixed air plus EGR zone. The three zones are too small to be resolved by the mesh and are therefore modeled as sub-grid quantities. The mixed zone is the result of turbulent and molecular mixing between gases in the other two zones and is where combustion takes place. The flame propagation phase is modeled by the flame surface density transport equation

incorporating the theoretical flame speed. Reitz and Diwakar model [21] accounts for the ‘bag break-up’, in which the non-uniform pressure field around the droplet causes it to expand in the low-pressure wake region and eventually disintegrate when surface tension forces are overcome and ‘Stripping break-up’, a process in which liquid is sheared or stripped from the droplet surface. Huh’s atomization model [22] is based on the gas inertia and the internal turbulence stresses generated in the nozzle. The ‘Bai’ spray impingement model [23] is formulated within the framework of the Lagrangian approach in order to reflect the stochastic nature of the impingement process, a random procedure is adopted to determine some of the droplet post-impingement quantities. This allows secondary droplets resulting from a primary droplet splash to have a distribution of sizes and velocities. Nitrogen oxides and soot are identified as main pollutants from this study. Three different mechanisms have been identified for the formation of nitric oxide during the combustion of hydrocarbons, namely thermal NO_x , prompt NO_x and fuel NO_x . Thermal NO_x is formed by high temperature oxidation of atmospheric nitrogen. Fuel NO_x is produced by the reaction of the nitrogenous components present in liquid or solid fossil fuel with oxygen. Prompt NO_x can be produced in significant quantities in certain combustion environments at low temperature, fuel-rich conditions and short residence times. The formation and emission of carbonaceous particles is based on the laminar flamelet concept in which all scalar quantities are related to the mixture fraction. The rates of soot formation can, however, be correlated with local conditions in diffusion flames or in partially premixed counter-flow twin flames.

The Computational Fluid Dynamics codes, es-ICE (Expert System for Internal Combustion Engines) and STAR-CD (Simulation of Turbulent flow in Arbitrary Regions – Computational Dynamics) are used to solve the discretized equations. The standard k - ϵ model with standard wall function has been employed for physical modeling. The program is based on the pressure-correction method and uses the algorithm formulated for Pressure Implicit Splitting of Operators (PISO). The first order upwind differencing (UD) scheme is used for the spatial discretisation of momentum, energy and turbulence equations with implicit temporal discretization. ECFM-3Z combustion model is used to characterize ignition and combustion. NO_x emission is modelled by using extended Zeldovich mechanism [24]. The soot emission model written in the Arrhenius single step form which considers the rate of change of soot mass is used to model soot emissions. The initial values of pressure and temperature are considered as homogeneous in the whole domain. The initial in-cylinder turbulent intensity is set at 10 % of the mean flow, and the integral length scale is set at 0.1 m. Temperatures at the cylinder head, the cylinder wall and the piston bowl that form the walls of the combustion chamber are specified as given in Table 3. Fuel injection is accomplished using Lagrangian multiphase droplets. Vertex data is used for interpolation method and under-relaxation factor of Lagrangian sources is set at 0.5. The droplet trajectory maximum file size is kept at 400 Mb, where maximum number of parcels are 500000. Turbulent dispersion, collision model and gravity effects for the droplets are taken into account. Wall heat transfer, thermal break-up and boiling effects are also considered when the droplet encounters the hot environment. $\text{C}_{14}\text{H}_{30}$ (N-Tetradecane) is selected as fuel from the National institute of standards and technology (NIST) table since it incorporates correct liquid fuel density. Huh atomization model is used. The injector nozzle L/D is chosen to be 6 and its coefficient of discharge is 0.7. Injection temperature is set at 310 K. The injector hole diameter is 0.4 mm and a separate lookup table is given to specify the injection timings with fuel injection quantity.

3. Problem Formulation

Re-entrant piston bowl is obtained by trimming the cylinder with a given spline for bowl. Here, due to the limitations in computing resources, 45 degree of the 3-D sector geometry is only selected for study. Radial, axial and piston top cells are selected appropriately and sector mesh is shown in Fig.1 for both TDC and BDC. Table 1. shows the engine in-cylinder data and fuel injection details. Table 2. shows the initial and boundary conditions that are set up in es-ICE CFD package. The computations are carried out by STAR-CD solver. The time accurate computations are performed in a Intel Xeon CPU (3.30 GHz, 3.24 GB RAM). The total elapsed CPU time is nearly 20 hours for a total of 4400 timesteps which leads to total time period of 20 milliseconds of 120° engine crank angle (from 680°CA to 800°CA). Fuel injection starts as 714°CA and stops at 722°CA . Auto-ignition in the cells takes place nearly at 719°CA corresponding to time-step around 1200. The problem for investigation is taken from Payri et al [9] and Jayashankara et al [17].

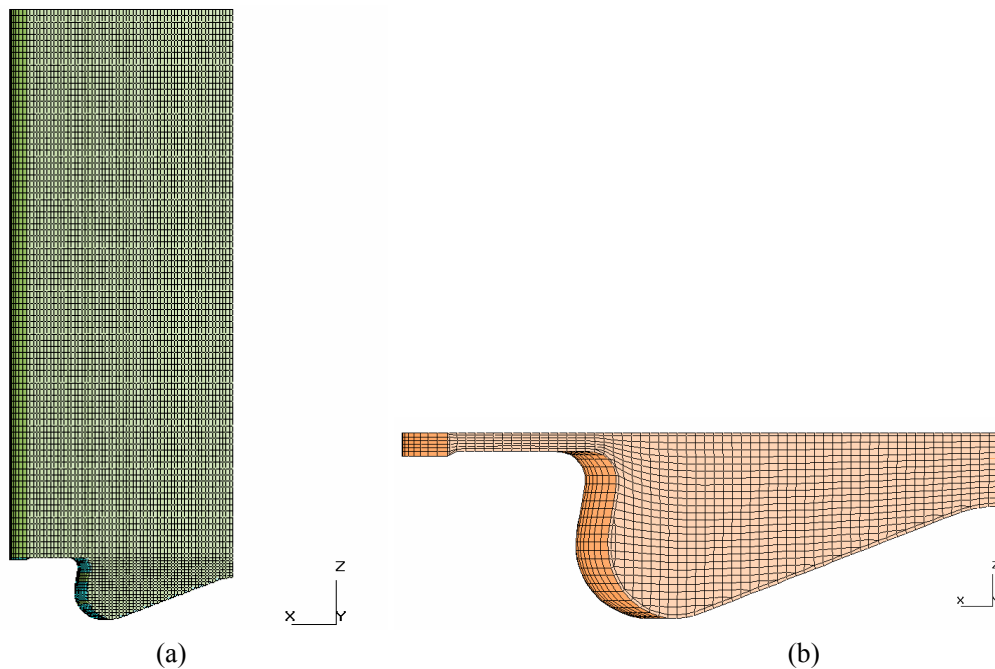


Figure 1: Computational domain of engine cylinder at (a) 800°CA and (b) 720°CA

4. Validation

The problem for validation is taken from the literature [20]. Table 3. shows the engine specifications for the problem to be validated with the CFD, ECFM-3Z model. Fig. 2 shows the comparison of simulated and experimental [16] in cylinder pressures and heat release rate for the direct injection diesel engine. Fig. 3 shows the spray from the injector towards the bowl. Once the convergence conditions are met, the computed in-cylinder pressure and heat release rates are checked and found to be in good agreement with the measured data. Time step independent tests (Fig. 4) and computational grid independency tests (Fig. 5). Crank angle step interval of 0.025°CA and mesh with 45000 cells at TDC position are selected as suitable values for further studies.

TABLE 1: ENGINE SPECIFICATIONS

Bore, Stroke	130 mm, 150 mm
Connecting Rod Length	275 mm
Compression Ratio	15.5
Engine Speed (N)	2000 RPM
Crank Angle Start	680 deg
Crank Angle Stop	800 deg
Fuel	n-Dodecane
Fuel injection quantity	207 mg/cycle
Start of Fuel Injection	6 deg bTDC
Fuel Injection Duration	8 deg

TABLE 2: INITIALIZATION AND BOUNDARY CONDITIONS

Cetane number	50
Swirl Ratio (SR)	1.4
Turbulence intensity	10 %
Equivalence ratio (EQR)	0.8
Exhaust gas recirculation	10 %
Combustion dome temperature	450 K
Piston crown temperature	450 K
Cylinder wall temperature	400 K
Pressure	9.5 bar
Temperature	550 K

TABLE 3: ENGINE SPECIFICATIONS FOR THE VALIDATION STUDY

Bore, stroke	0.085 m, 0.088 m
Connecting rod length	0.145 m
Injector hole diameter	148 x 10 ⁻⁶ m
Spray Angle	152 deg
Speed	1640 rpm
Start of injection (deg bTDC)	6
Injection duration (deg)	8.03
Injected mass (g)	0.0144
F/A equivalence ratio	0.67
EGR rate (%)	31
Swirl ratio	2.8

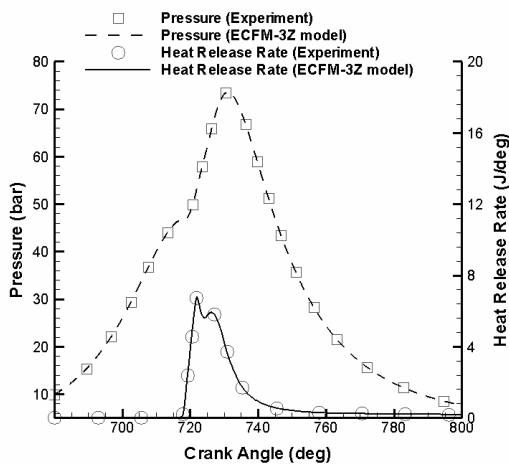


Figure 2: Validation of pressure and heat release rates [17]

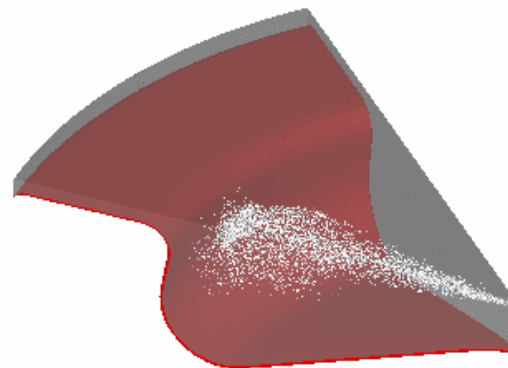


Figure 3: Fuel spray at TDC (720 deg CA)

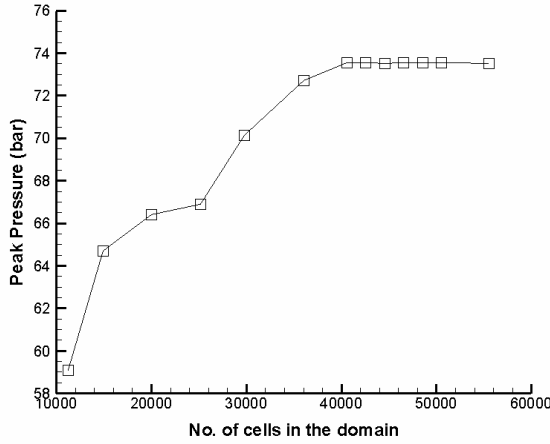
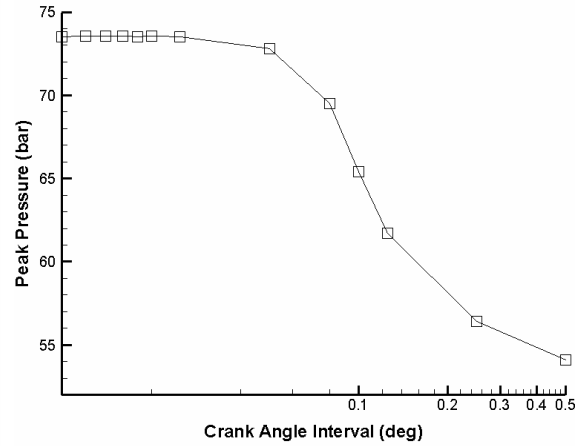


Figure 4: Grid independent study



$$\text{Tumble} = \frac{\sum_{\text{Cells}} \rho V [(y_i - y_m)w_i + (z_i - z_m)v_i]}{2\pi \frac{N}{60} \sum_{\text{Cells}} \rho V [(y_i - y_m)^2 + (z_i - z_m)^2]} + \frac{\sum_{\text{Cells}} \rho V [(x_i - x_m)w_i + (z_i - z_m)u_i]}{2\pi \frac{N}{60} \sum_{\text{Cells}} \rho V [(x_i - x_m)^2 + (z_i - z_m)^2]}$$

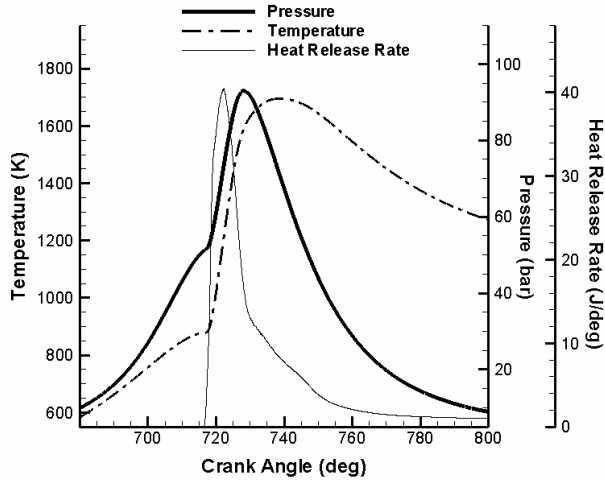


Figure 6: Cylinder averaged pressure, temperature and heat release rate

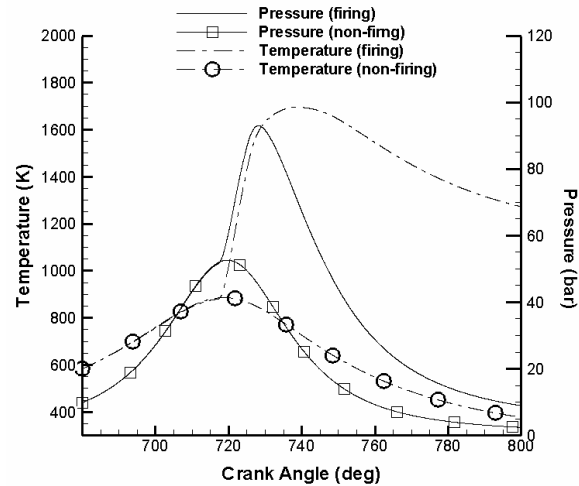


Figure 7: Cylinder averaged pressure and temperature for firing and non-firing conditions

Variation of turbulent intensity for different swirl ratio during the closed-valve duration is shown in Fig. 11. It is observed that swirl ratio of 4.1 is 12% higher at TDC as compared to swirl ratio of 1.4. The peak pressures, temperatures and heat release rates are increasing with swirl ratio as shown in Fig. 12. This is due to the increase in turbulent intensity and decreasing ignition delay. This is achieved due to rapid (highly turbulent) mixing of fuel vapor and air in the cylinder. By varying the swirl ratio from 1.4 to 4.1, the peak pressures, peak temperature, peak heat release rates increase by 7 %, 8.6 % and 31 % respectively. The longer ignition delay leads to slow burning rate, resulting in lower pressure and temperature inside the cylinder. Hence, most of the fuel burns under diffusion combustion mode at lower swirl ratio. The accumulation of evaporated fuel is relatively less resulting in shorter ignition delay for higher swirl ratio. The shorter ignition delay leads to rapid burning rate and sudden rise in pressure and temperature. Hence, most of the fuel burns in premixed mode rather than diffusion mode resulting in higher peak heat release rate and shorter combustion duration. Soot and NO_x emissions are shown in Fig. 13 and the corresponding contours are shown in Fig. 14 and Fig. 15. Soot decreases as there is a chance of favorable mixing of fuel vapor and air at increasing swirl ratio. However, due to increase in the in-cylinder temperature, NO_x emissions increases with increasing swirl. This is justified by the contours of temperature observed in Fig. 16. The ECFM – 3Z combustion model is coupled with improved burned gas chemistry that allows CO , soot, and NO_x formation calculations. The principle effect of turbulence is to increase the flame surface area. By increasing the swirl ratio 1.4 to 4.1, peak soot level reduction by 38 % but peak NO_x emissions increased by 24 %.

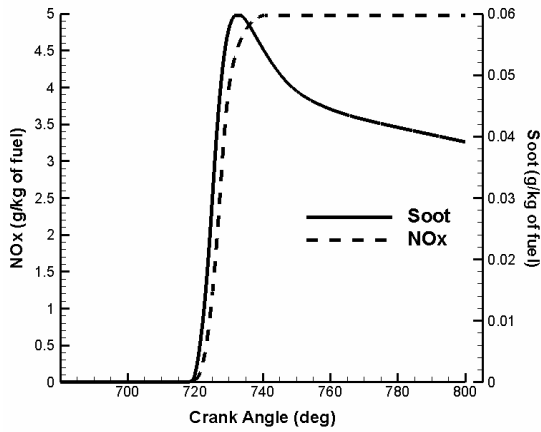


Figure 8: Cylinder averaged NOx, soot emissions

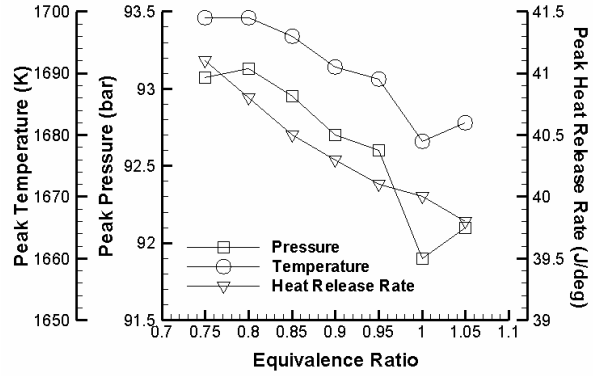


Figure 9: Peak values of pressure, temperature heat release rates for different equivalence ratio

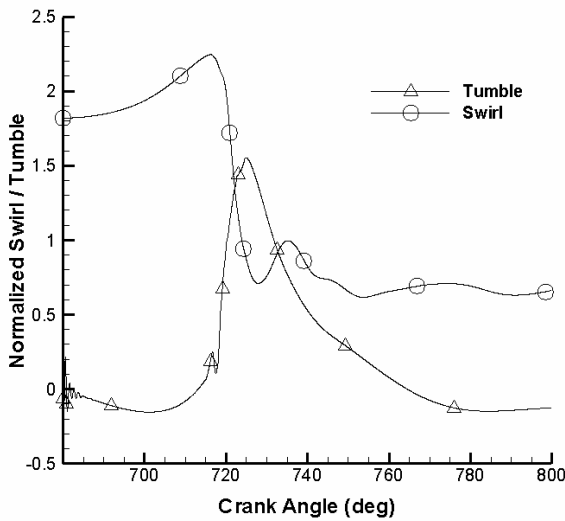


Figure 10: Swirl and tumble at different crank angles

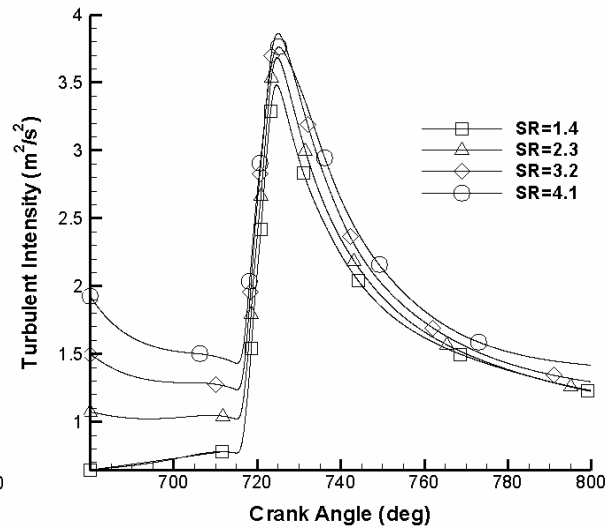


Figure 11: Turbulent Intensity for different swirl ratio (SR)

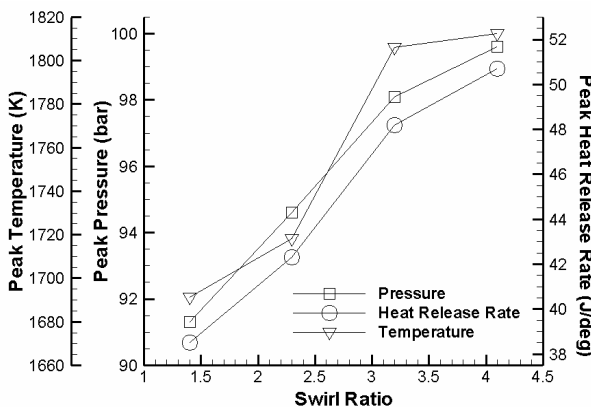


Figure 12: Peak pressure, temperature and heat release rates for different swirl ratio

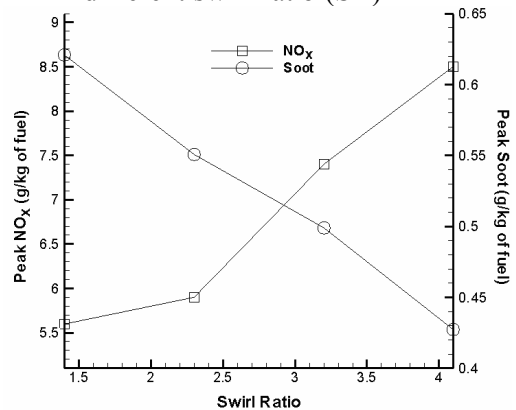


Figure 13: Peak NO_x, soot emissions for different swirl ratio

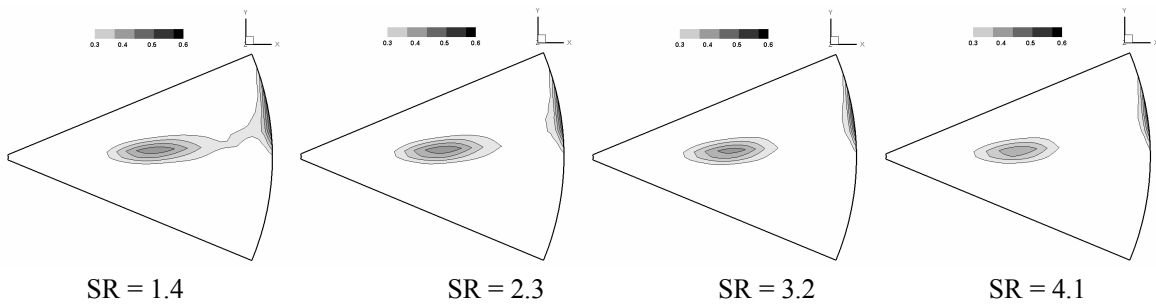


Figure 14: Contours of soot emissions (g/ kg of fuel) for different swirl ratio (SR) at TDC

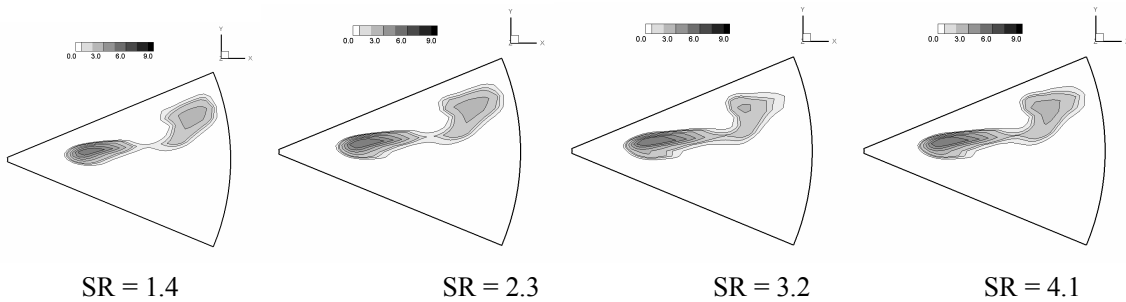


Figure 15: Contours of NO_x emissions (g/ kg of fuel) for different swirl ratio (SR)

6. Conclusions

In the present work, ECFM-3Z model is used to model the combustion and emission in direct injection diesel engine for various equivalence and swirl ratio. Validation studies indicate there is a close match in results between CFD (ECFM-3Z model) and experiments. The flame surface density and reaction variable contours show that reaction sites are phenomenological between 1.4 and 4.1 swirl ratio.

From the present study, it is found that

- The peak heat release rate decreases with increasing equivalence ratio from 0.75 to 1.05.
- Turbulent intensity at TDC is increased by 12 % from swirl ratio of 1.4 to 4.1.
- By varying the swirl ratio from 1.4 to 4.1, the peak pressures, peak temperature, peak heat release rates increase by 7 %, 8.6 % and 31 % respectively.
- By increasing the swirl ratio from 1.4 to 4.1, peak soot level reduces by 30 % but peak NO_x emissions increases by 54 %.

The increase in NO_x emissions can be reduced by employing the concept of exhaust gas recirculation in the engine cylinder. This feature is taken in the ECFM-3Z model and will be studied in the future.

References

- [1] Moparthy, A., R. Das, R. Uppaluri, S.C. Mishra, Optimization of heat fluxes on the heater and the design surfaces of a radiating-conducting medium, Numerical Heat Transfer: Part Applications, 2010. 56 (10): p.846-860.
- [2] Zhou, H., K. Cen, J. Fan, Multi-objective optimization of the coal combustion performance with artificial neural networks and genetic algorithms, International Journal of Energy Research, 2005. 29 (6):p.499-510.

- [3] Das, R., Inverse analysis of Navier-Stokes equations using simplex search method, *Inverse Problems in Science and Engineering*, 2012. 20 (4): p. 445-462.
- [4] Wickman, D., P. Senecal, R. Reitz, Diesel engine combustion chamber geometry optimization using genetic algorithms and multi-dimensional spray and combustion modeling, SAE Paper No. 2001-01-0547.
- [5] Zhang, L., Ueda, T. Takatsuki, T. Yokota., A study of the effects of chamber geometries on flame behaviour in a direct injection diesel engine. *SAE Paper No. 952515*.
- [6] Stephenson, P.W., Claybaker, P.J., Rutland, C.T., Modeling the effects of intake generated turbulence and resolved flow structures on combustion in direct injection diesel engine. *SAE Paper No. 960634*.
- [7] Bianchi G.M., S. Fontanesi, On the applications of low-Reynolds cubic $k-\epsilon$ turbulence models in 3D simulations of ice intake flows. *SAE Paper No. 2003-01-0003*.
- [8] Chen, A., A. Veshagh, S. Wallace, Intake flow predictions of a transparent direct injection diesel engine. *SAE Paper No. 981020*.
- [9] Payri, F., J. Benajes, X. Margeo, A. Gil, CFD modeling of the in-cylinder flow in direct-injection diesel engine. *Computers & Fluids*; vol(33), 2004, p. 995–1021.
- [10] Auremma, M., F.E. Corcione, R. Macchioni, G. Valentino, Interpretation of air motion in reentrant bowl in-piston engine by estimating Reynolds stresses. *SAE Paper No. 980482*.
- [11] Brandl, F., W. Reverencic, Cartellieri, J.C. Dent, Turbulent air flow in the combustion bowl of a DI diesel engine and its effect on engine performance. *SAE Paper 790040*.
- [12] Arcoumanis C., A.F. Bicen, J.H. Whitelaw, Squish and swirl-squish interaction in motored model engines. *ASME J Fluid Mech* :vol(105),12, 1993.
- [13] Kondoh T., A. Fukumoto, K. Ohsawa, Y. Ohkubo, An assessment of a multidimensional numerical method to predict the flow in internal combustion engines. *SAE Paper 850500*.
- [14] Saito T., Y. Daisho Y, N. Uchida, N. Ikeya, Effects of combustion chamber geometry on diesel combustion. *SAE Paper 861186*.
- [15] C. D. Rakopoulos, G.M. Kosmadakis, E.G. Pariotis, Investigation of piston bowl geometry and speed effects in a motored HSDI diesel engine using a CFD against a quasi-dimensional model. *Energy Conversion and Management*; vol(51),3,2010, p 470–84.
- [16] Jaeman L., M. Kyoungdoug, The effects of spray angle and piston bowl shape on diesel engine soot emissions using 3-D CFD simulation. *SAE Paper 2005-01-2117*.
- [17] Jayashankara, B., V. Ganesan, Effect of fuel injection timing and intake pressure on the performance of a DI diesel engine – A parametric study using CFD, *Energy Conversion and Management* vol (51), 2010 pp 1835–1848.
- [18] Prasad, B.V.V.S.U., C.S. Sharma, T.N.C Anand, R.V. Ravikrishna, High swirl-inducing piston bowls in small diesel engines for emission reduction, *Applied Energy*, vol(88), 2011, p2355–2367.
- [19] es-ICE user guide, version 4.16.001, *CD-adapco*, 2011.
- [20] Colin, O., A. Benkenida, The 3-Zones Extended Coherent Flame Model for computing premixed & diffusion Combustion. *Oil & Gas Science and Technology, Rev. IFP*, vol (59),6,2004, p 593-609.
- [21] Reitz R.D., R. Diwakar, Effect of drop breakup on fuel sprays, SAE Technical Paper Series 860469 (1986).
- [22] Huh K.Y., A.D. Gosman, A phenomenological model of Diesel spray atomisation', Proc. Int. Conf. on Multiphase Flows (ICMF '91), Tsukuba, 24-27 September (1991).
- [23] Bai C., A.D. Gosman, Mathematical modeling of wall films formed by impinging sprays, SAE Technical Paper Series 960626 (1996).
- [24] Flower, W.L., R.K. Hanson, C.H. Kruger, Kinetics of the reaction of nitric oxide with hydrogen, 15th Symp. (Int.) on Combustion, The Combustion Institute, 1975, pp. 823-832.